In: Virtual Reality
Editor: Nada Bates-Brkljac,
ISBN: 978-1-61470-246-7

Chapter 3

REVERSE ENGINEERING TOOLS IN AUGMENTED REALITY TO SUPPORT ACQUISITION, PROCESSING AND INTERACTIVE STUDY OF CULTURAL AND ARCHAEOLOGICAL HERITAGE

Pier Paolo Valentini*
Department of Industrial Engineering
University of Rome "Tor Vergata"
Via del Politecnico, 1
00133 – Rome, Italy.

ABSTRACT

This chapter deals with the description of recent developments concerning with both hardware and software implementation for supporting reverse engineering procedures by using an augmented reality environment. The discussed investigation is mainly focused on applications in the study of cultural and archaeological heritage. The use of augmented reality for engineering purposes allows the development of specific analysis tools in which the computer graphics supports the user with virtual contents that are included and harmonized in a real context. For the specific reverse engineering implementation, thanks to this integration, it is possible to perform interactive shape acquisition, geometrical analyses and assisted reconstruction of shards being supported by efficient computer aided tools and three dimensional computer graphics. The chapter begins with a brief introduction on the use of virtual environments for supporting the visualization and the sharing of cultural and archaeological heritage. In a second part, a detailed description of both hardware and software implementations is presented. In a third part, the integration of the reverse engineering algorithms and methodologies is addressed together with some examples of application.

* valentini@ing.uniroma2.it

1. INTRODUCTION

During the last decades, the implementations of computer-aided methodologies have revolutionized many fields of the human knowledge. Thanks to the increasing of computational and graphical performances, many activities have been simplified and new methodologies to approach and solve problems have been developed. In particular, the scientific literature reports many contributions about the successful use of computer graphics (CG) and computer-aided design (CAD) supporting the investigation of archaeological finds, their classification and, in particular way, their visualization. Starting from the results of these promising methodologies, a new discipline has born: the *virtual archaeology* [1]. Although there are many applications and specific implementations, this new discipline bases its innovative idea on the use of computer graphics in particular and computer-aided tools in general to support the work of archeologists and experts in the study, reconstruction and dissemination of historical and artistic objects [2-9].

One of the main applications of the virtual archaeology is about the building of virtual museums in which the presence of physical objects is replaced with virtual replicas projection. After an initial effort to prepare the virtual contents by digitization of the shapes, the exhibitions can be set up with lower costs than the real ones and the limited presence of real objects reduces the risk of wear and damage. Another important advantage of virtual museums is the possibility to disseminate the contents overtaking the limits imposed by geographic distance and to organize simultaneous exhibitions in different locations. Moreover, the visualization of virtual objects allows to investigate and appreciate several aspects which cannot be observed on the real ones. A virtual replica of a physical object allows the visualization from different points of view, animations, entire scenarios reconstruction, augmented visual information about related historical, cultural and technological aspects. The main challenge of these methodologies is about the increase of realism in order to reduce the gap between the appearance of digital and physical objects.

The most of CG applications in archeological heritage concerns with the use of Virtual Reality (VR) which allows visual experiences, displaying a fully virtual environment (both background and additional objects) either on an external computer screen (non immersive) or through stereoscopic head mounted displays (immersive). In some applications the visual experience is enhanced with the use of additional sensory information, such as sound through speakers or headphones.

Figure 1 shows an example of a fully virtual museums environments built with computer graphics methodologies and used for VR implementation.

During the last years, another important methodology, based on the realistic visualization of virtual contents, has been developed: the *Augmented Reality* (AR) [10]. AR is a field of Computer Vision (CV) concerning with the techniques for projecting virtual contents in a scene with real objects, creating the illusion of a unique real environment [11-13]. This approach is different from VR where all the objects and background in the scene are virtual. In order to achieve an adequate level of realism in AR applications, it is important a real-time computation of the relative position between the user and the scene and precise collimation and registration between real and virtual objects. The augmented scene (i.e. the scene with both virtual and physical objects) is then projected back to the user by means of head mounted displays. Virtual objects in the scene can be complex tridimensional static or animated shapes, simple text, graphs or visual information.

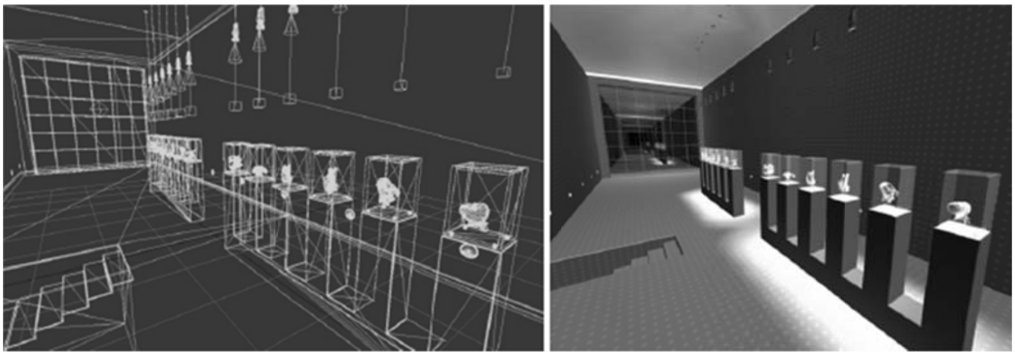

Figure 1. Building a fully digital environment for a virtual museum using computer graphics methodologies.

There are many advantages in the use of Augmented Reality with respect to Virtual Reality. First of all, it is not necessary to virtually reproduce all the objects to include in the scene. Moreover, the user is more at ease because he recognizes a background and a scene that is more familiar involving real objects. And again, an AR implementation can be often achieved using devices with more affordable costs with respect to those used in VR.

The increasing interest for the Augmented Reality and its applications in many fields is testified by several scientific papers. The AR has been used in medicine and surgery [14], robotics [15], maintenance and assembling activities [16-19], architecture [20], e-learning [21-22], manufacturing [23-24], services and logistics [25-26], navigation [27], etc. Recently the Augmented Reality has been also used for developing many engineering design tools as modelling and simulation environments [28-29].

Other recent papers have underlined the increasing interest for the implementation of augmented museums, where the real and the virtual artifacts can be arranged in harmony [30-31]. These applications have often the disadvantage that the user may only visualize pre-computed contents with a limited interaction.

The recent developments of both hardware and software performance suggest to increase the level of interaction between the user and the scene changing the user's role from spectator to actor. The main idea to overcome this limitation is to use the AR methodologies for going beyond a mere visual or acoustical experience, including an high level of user interaction. Moreover, this combination between visualization and interaction can be a solid base for developing specific computer aided tools for supporting the study and the review of archeological objects.

One of the most important computer aided tool in archaeology is the Reverse Engineering (RE). RE is a combination of measurements and procedures for reconstructing and analyzing mathematical and topological models of real shapes. By this way, it is possible to study the interesting object using mathematical models, being more precise, objective and speeding up all the investigation phases.

Generally speaking, a RE process involves a first phase of acquisition and measurement on the physical object. This phase is performed by means of specific devices. Some of them require the contact with the object (i.e. coordinate measuring machines, instrumented arms, etc.). Some others work without touching the real objects by means of optical triangulation methods (laser scanners), magnetic field perturbation, acoustic reflection, etc. The results of acquisition is, in general, a collection of points coordinates. Subsequently, this information has to be processed and analyzed in order to produce a mathematical representation useful for both modeling and interrogation issues. One of the possible computer-aided investigation is the automatic (or assisted) extraction of the geometrical, morphological and functional information from 3D acquired surfaces which is useful for obtaining both global and local information. Global information is related to the modelling of the entire shape and it is useful for building virtual replicas suitable for Augmented or Virtual Reality implementations (i.e. for the building of virtual exhibitions). Local information concerns with the geometrical attributes of the single point or curve with are essential for any subsequent analysis and classification. Figure 2 shows an example of a real vase and a virtual replica built from a laser scanner acquisition and a computer-aided surface fitting.

Starting from this background and these motivations, the chapter deals with the description of recent developments of both hardware and software tools in order to implement innovative methodologies based on the use of augmented reality to support the tasks of acquisition, processing and study of archeological finds. By the combined use of image processing, computer graphics, reverse engineering and augmented reality, it is possible to implement useful tools for enhancing and support the study of archaeological heritage, integrating analysis and classification procedures, with visualization in a mixed environment.

Figure 2. An example of a real vase (on the left) and its virtual replica built from a laser scanner acquisition (on the right).

The first part of the chapter focuses on the integration of reverse engineering methodologies in the augmented reality environment. This combination is very important to reproduce accurate three dimensional virtual replicas and perform interactive visualization. The second part concerns with the development of interactive analysis tools for performing geometrical investigations and interrogation on virtual shapes and with their visualization on the augmented scene. The third part deals with the development of methodologies for the interaction among virtual and real objects and the assisted reconstruction of full part from fragments.

2. HARDWARE AND SOFTWARE SETUP

A general augmented reality implementation needs devices for acquiring a video stream from a real scene, a processing unit for decoding and analyzing the acquisition and rendering the augmented scene, and devices for projecting it back to the user. In order to ensure an high level of interaction other devices for tracking user's position and interpret his intent have to be included and integrated in the whole system. For the specific purpose of this investigation, the implemented AR system (depicted in Figure 4) is based on that proposed in [29] and it is comprised of:

- one input video device Microsoft LifeCam VX6000 USB 2.0 camera, able to catch frames up to 30 Hz with a resolution of 1024x768 pixels;
- one Head Mounted Display equipped with OLed displays (Z800 3D visor by Emagin - http://www.3dvisor.com/);
- one personal computer with an Intel Core 2 Quad-core processor, 3 Gb RAM and a NVidia Quadro FX3700 graphic card.

In order to achieve an interactive application, a tracking device has to be included in the system. This device must also to be suitable to perform user-assisted shape acquisition for reverse engineering purposes.

Previous investigations have dealt with possible solutions involving electromagnetic devices [28] or optical markers [19, 29]. Both these instrumentations have some limitations and seem inappropriate for the purpose of this investigation. On the one hand, electromagnetic trackers are precise but they are very sensible to the perturbation of the magnetic field which may produces inaccurate acquisitions. Archaeological finds often include metallic parts or ferromagnetic powder which cause inacceptable perturbation of the magnetic field. On the other hand, optical markers are less precise but are insensitive to material composition. Moreover, a continuous acquisition requires that the markers have to be always visible to the camera and this may limit the traceable movement and the working space. The accurate reverse engineering acquisition and post processing of the real shapes need a very precise position tracking that cannot be ensured by these simple optical means. For all these reasons, for tracking the user in the scene, the augmented reality system has been integrated with:

- one Revware Microscribe GX2 (http://www.revware.net/microscribe_g.asp).

The Microscribe GX2 is an instrumented arm digitizer able to a real-time acquisition of position and attitude of a stylus end-effector with a precision of ±0.2 mm in a working space of about 1.2 m of diameter. Moreover it has been successfully used in many user-assisted reverse engineering procedures.

The complete implemented hardware system is depicted in Figure 3.

In order to integrate the use of the digitizer in the augmented reality application, the information coming from its acquisition has to be real time computed and synchronized to the augmented reality computational sequence.

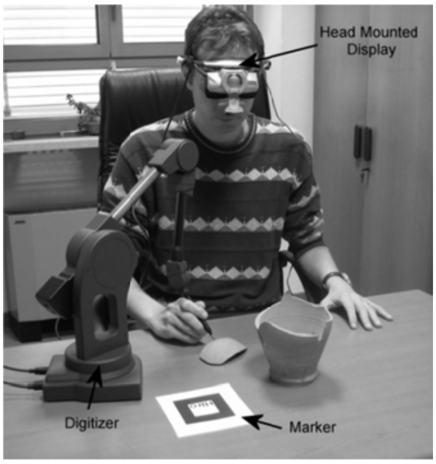

Figure 3. Hardware implementation for the investigation.

For this purpose each frame acquisition, the position and attitude of the digitizer end-effector has to be acquired in order to achieve a time synchronization. Then, two parallel processes starts. On the one hand, the acquired frame is processed for detecting the presence of patterned makers to compute the projection matrix that represent the user's perspective point of view in the scene. On the other hand, the information coming from the digitizer is processed in order to track the user's position in the scene, interpret his intent and compute modelling or analysis results. The acquisition of the digitizer has to be related with the user's point of view in order to achieve a spatial collimation of data. This feature is very important for the correct rendering of virtual contents (both virtual shapes and analysis results) that are projected back to the user and superimposed to the acquired image of the real scene. Figure 4 shows a scheme of the overall process. Details of collimation between digitizer acquisition and augmented scene, together with modeling and analysis issues will be discussed in details in the next sections.

All the supporting software has been implemented using C++ programming language and Microsoft Visual Studio 2003 developing suite. Routines for image processing have been developed using the open source library named ARToolkit which has been successfully used in other investigations. It can be freely downloaded from http://sourceforge.net/project/showfiles.php?group_id=116280. It comprises a set of numerical procedures which are able to detect and recognize planar patterned marker in a video stream in real time. Using correlation techniques, the routines are also able to compute relative position and attitude between markers and camera with good precision for visual purposes. This computation is necessary for an accurate perspective collimation between virtual entities and real scene. The details about specific implementation and about the contents of the library go beyond the scope of this paper and the interested reader can find useful material and specific documentation on the internet site http://www.hitl.washington.edu/artoolkit/.

The Microscribe GX2 has been integrated using the Microscribe SDK library that allows the real time access to position and attitude of each link of the instrumented arm.

For managing complex geometries the Open Vrml library has been included (freely downloadable from http://openvrml.org/). All rendering tasks about virtual objects in the augmented scene have been performed using OpenGL library. All these pieces of software have been integrated into a single simulation environment as shown in Figure 5.

All the procedures for shape modelling, interrogation, analysis and manipulation have been written by the author for the specific purpose of this investigation. Details about these subroutines will be provided in the next sections of the chapter.

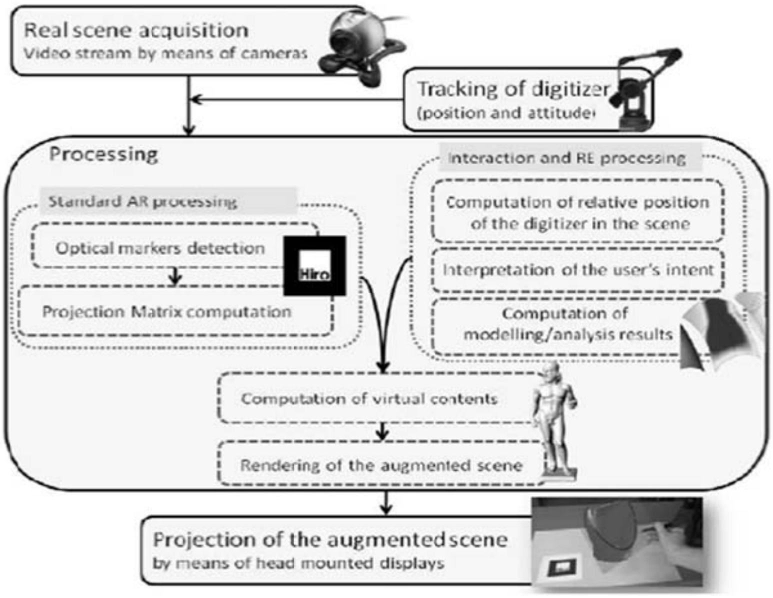

Figure 4. Functional scheme of the proposed interactive augmented reality application.

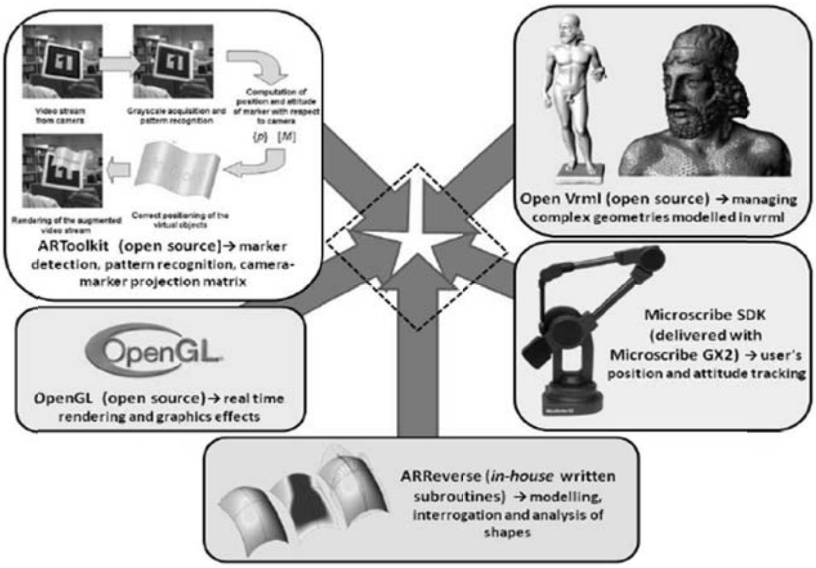

Figure 5. Interaction among libraries for the developing of a software application and for managing all the devices.

2.1. Collimation between Measurement and Visualization

The first step in the integration of the digitizer in the augmented scene is the collimation between the information acquired by the instrumented device and that coming from the digital camera. The video stream acquired by the digital camera is elaborated by an image processing routine. This procedure is able to recognize a patterned marker in the scene and to compute the corresponding transformation matrix $\left[T_{word}^{camera}\right]$ between the camera and the real word. This matrix is used to project all the virtual contents in the augmented scene in the correct position and perspective.

The information acquired by the digitizer concerns with the position and attitude of the end effector with respect to the reference frame fixed to the device itself.

In order to ensure the collimation between the data steam coming from the camera and that from the digitizer, it is important to compute the relative transformation matrix $\left[T_{word}^{digitizer}\right]$ between the digitizer and the world (the marker). This calibration has to be performed only at the beginning of the application and it has to be repeated only if the relative position between the marker and the digitizer changes.

The calibration procedure can be performed by picking with the digitizer a set not-aligned points (four no-coplanar points at least) at known positions with respect to the relative frame associated to the marker.

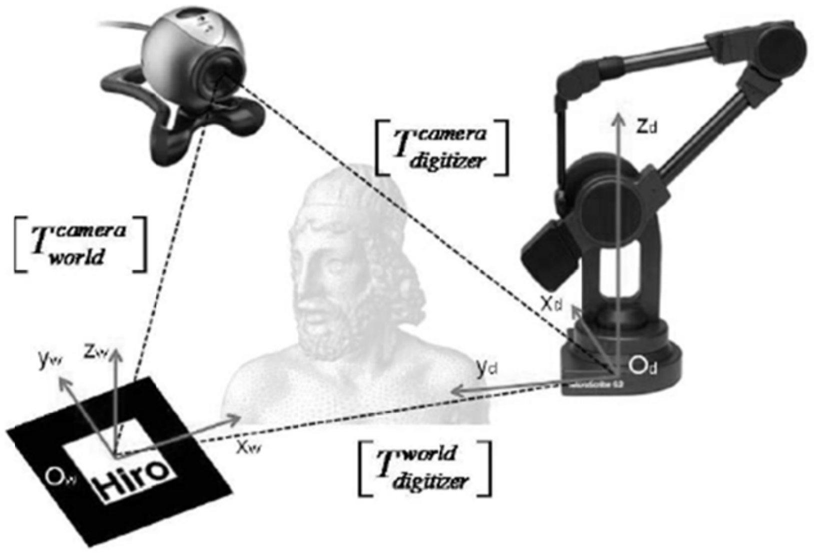

Figure 6. Relative transformations among camera marker (world) and digitizer.

For expressing coordinate transformation between points it is useful to deal with homogeneous transformation matrices which include information on both rotation and translation parameters. A generic homogeneous transformation matrix can be expressed in the form:

$$[T] = \begin{bmatrix} [\text{Orientation}]_{3\times3} & [\text{Position}]_{3\text{x}1} \\ 0 \quad 0 \quad 0 & 1 \end{bmatrix} \tag{1}$$

In the same way the generic point P can be expressed with the following coordinate vector:

$$\{P\} = \{x \quad y \quad z \quad 1\}^T \tag{2}$$

The coordinate transformation of a generic point P from the local coordinate system of the digitizer to the world coordinate system related to the marker can be written as:

$$\{P\}_{world} = \left[T_{world}^{digitizer}\right]\{P\}_{digitizer} \tag{3}$$

where:

$\{P\}_{world}$ is the vector containing the coordinate of the point P expressed in the world reference frame;

$\{P\}_{digitizer}$ is the vector containing the coordinate of the point P expressed in the local reference frame (digitizer).

Considering a collection of points $P_1 \quad P_2 \quad \ldots \quad P_n$, we can built two matrices as:

$$[P]_{world} = \left[\{P_1\}_{world} \quad \{P_2\}_{world} \quad \cdots \quad \{P_n\}_{world}\right] \tag{4}$$

$$[P]_{digitizer} = \left[\{P_1\}_{digitizer} \quad \{P_2\}_{digitizer} \quad \cdots \quad \{P_n\}_{digitizer}\right] \tag{5}$$

In order to compute the matrix $\left[T_{word}^{digitizer}\right]$ we have to solve the system of equations

$$[P]_{world} = \left[T_{world}^{digitizer}\right][P]_{digitizer} \tag{6}$$

for the unknown elements of the matrix $\left[T_{word}^{digitizer}\right]$. An homogeneous transformation matrix is defined by 6 independent parameters (three for the description of the rotation and three for the translation). For this reason, the system (6) has more equations than unknowns and the solution can be computed as:

$$\left[T_{world}^{digitizer}\right] = [P]_{world}^{-1^+}[P]_{digitizer} \tag{7}$$

where the $[P]_{world}^{-1^+}$ denotes the pseudo-inverse matrix of the $[P]_{world}$ matrix.

Due to numerical approximation or errors in measurement, the orientation block of the computed matrix $\left[T_{word}^{digitizer}\right]$ can result not exactly orthogonal. Since it represents a rigid spatial rotation, it is important to correct this imprecision. For this purpose, we can operate a QR decomposition of this orientation block:

$$\left[Orientation_{word}^{digitizer}\right]_{3x3} = \left[R_1\right]_{3x3}\left[U_1\right]_{3x3} \quad (8)$$

where (due to the QR algorithm):

$\left[R_1\right]$ is an orthogonal matrix representing the corrected rotation and $\left[U_1\right]$ is a matrix whose upper band contains the errors of approximation and the lower band has only zero elements. In case of a pure rotation (orientation block without errors) $\left[U_1\right] = \left[I\right]$.

In order to compute the transformation matrix between the digitizer and the camera $\left[T_{camera}^{digitizer}\right]$, useful to collimate the acquired points to the visualized ones, a matrix multiplication has to be performed:

$$\left[T_{camera}^{digitizer}\right] = \left[T_{word}^{digitizer}\right]\left[T_{camera}^{word}\right] . \quad (9)$$

3. Interactive Study of Real Objects

An accurate study of the real archaeological objects requires geometrical and morphological analysis of the corresponding shapes. In order to process these components, the real geometrical features have to be traduced into a mathematical representation suitable for computational purposes. The activities related to the building of mathematical representation of real shapes are often addressed as reverse engineering (RE) methodologies. The most of RE methodologies begins from the acquisition of a collection of points on the surface of the interesting object. In a second phase, these points can be connected in the right order in order to form a network of curves sketched on the acquired surface. In a third phase, the network of curves can be used to build a mathematical representation of an interpolated surface (Figure 7).

By the combination of reverse engineering techniques and augmented reality, it is possible to implement the basic reverse engineering procedures in an interactive environment where the user can built the mathematical representation and graphical rendering of curves and surfaces directly on the real shape.

The high level of interaction that can be reached by this integration is very important especially in those fields where the contribution of an expert user is crucial. The use of augmented reality gives the opportunity to sketch and visualize the geometrical entities directly on the real objects using three dimensional graphics. By this way, the building of geometrical entities can be guided by the user and assisted by computer aided tools and can be performed with a continuous reference to the real shapes. Thanks to the use of a precise mechanical digitizer, the drawing of these entities can be made with a tool similar to a pen that can easily manipulated in space.

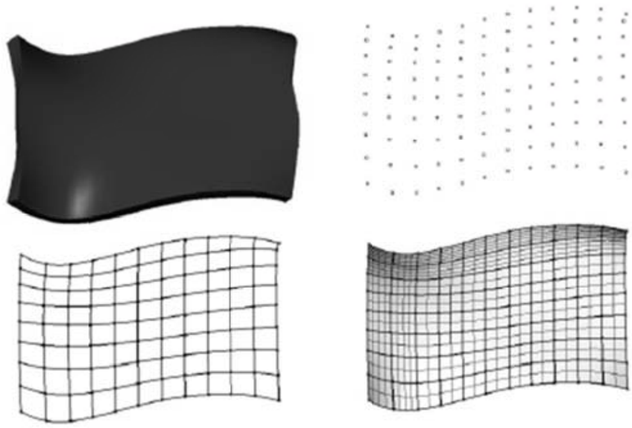

Figure 7. Reverse engineering of the shape of a real object: starting from the real surface (top, on the left), a set of points can be acquired (top, on the right); from these points a network of curve can be built (bottom, on the left) and then a surface patch can be generated (bottom, on the right).

The mathematical representation of real shape can be very useful for archaeological investigations. Many classification criteria are based on the interrogation and the comparison of the profiles, typologies, patterns and textures [33-35]. Moreover, a geometrical model helps to apply computational algorithms for a more precise correlation among shapes and allows objective and repeatable evaluations.

Before describing the details of the possibilities and the implementations of the interactive study of archeological objects some recalls of computer aided geometrical design [36] are required.

3.1. Brief Recalls on Curves and Surfaces Representation

In computer-aided design, one of the most suitable tool for built a curve interpolating a given set of points is the B-spline structure. It is a very common tool implemented in many computer aided design applications. Generally speaking, a spline is a mathematical representation of a curve that approximates or interpolates a given set of points. One of the most used spline representation is the Bézier-like form. Following this approach, an entire curve is split into several shorter Bézier curves that are sequentially connected with an appropriate smoothness and geometrical continuity. A generic Bézier curve $p(u)$ fitting a given set of m control points $\{P_0 ... P_{m-1}\}$ can be expressed in a parametric form as:

$$p(u) = \sum_{i=0}^{m-1} b_i(u) P_i \tag{10}$$

where $b_i(u)$ are the blending functions (piecewise polynomial functions of the variable *u*). In general, the blending functions depend on the degree of the interpolating polynomials. It is important to notice that, chosen the degree of the blending functions, one can use a small set of points to describe a complex curve shape. Moreover, following the reverse approach, one can use a small set of points to built a complex curve obtaining an exact mathematical representation for further computations.

In order to simplify the evaluation of local geometrical properties of a curve (e.g. tangent vector, curvature, etc.) it is useful to introduce the Frenet frame, which is a local frame moving along the curve. Assuming that the curve is given in the algebraic form as in Eq. (10), the versors associated with the Frenet coordinate system can be expressed as follows:

$$t(u) = \frac{p'(u)}{\left\| p'(u) \right\|} \quad \text{is the tangent unit vector} \tag{11}$$

$$m(u) = b(u) \times t(u) \quad \text{is the normal unit vector} \tag{12}$$

$$b(u) = \frac{p'(u) \times p''(u)}{\left\| p'(u) \times p''(u) \right\|} \quad \text{is the binormal unit vector} \tag{13}$$

where:

$$p'(u) = \frac{\partial p(u)}{\partial u} \text{ and } p''(u) = \frac{\partial^2 p(u)}{\partial u^2}$$

Considering the changing of the Frenet frame along the curve, it is possible to define two scalar parameters: the Frenet curvature $\kappa(u)$ and the Frenet torsion $\tau(u)$:

$$\kappa(u) = \frac{\left\| p'(u) \times p''(u) \right\|}{\left\| p'(u) \right\|^3} \tag{14}$$

$$\tau(u) = \frac{\left(p'(u) \times p''(u) \right) \cdot p'''(u)}{\left\| p'(u) \times p''(u) \right\|^2} \tag{15}$$

For the representation of the surfaces, the approach is similar. A surface can be reviewed as a piecewise interpolating function of two variables. In this case the interpolation is among a collection of *m* x *n* control points $\{\mathrm{P}_{ij}\}$ (control points net). The surface can be expressed in the parametric form as:

$$s(u,v)=\sum_{i=0}^{m-1}\sum_{j=0}^{n-1}b_i(u)b_j(v)\mathrm{P}_{ij} \tag{16}$$

where $b_i(u)$ and $b_j(v)$ are the blending functions (piecewise polynomial functions of the variables *u* and *v*, respectively) fitting the control points.

As for the curve, for each point of a surface it can be defined a reference frame with the following versors:

$$t_1=\frac{s_u}{\|s_u\|} \quad \text{is the first tangent unit vector} \tag{17}$$

$$t_2=\frac{s_v}{\|s_v\|} \quad \text{is the second tangent unit vector} \tag{18}$$

$$n=\frac{s_u\times s_v}{\|s_u\times s_v\|} \quad \text{is the normal unit vector} \tag{19}$$

where $s_u=\frac{\partial s(u,v)}{\partial u}$ and $s_v=\frac{\partial s(u,v)}{\partial v}$.

The details about the definition of blending functions, their practical computation and the particular way to interpolate points and curve network go beyond the scope of this chapter. An interested reader can find useful material in [36-37].

3.2. Acquisition of Curves and Surfaces of Archeological Fragment

The first step in the interactive study of the archaeological finds is the acquisition of the shapes and their mathematical representation. This activity can be performed using the mechatronic digitizer and picking a set of *m* $\{L_j\}$ points directly on the surface of the interesting object. These points can be used of the real time building of spline curves using the representation in Eq. (10). The only difference is that that points $\{\mathrm{P}_0...\mathrm{P}_{m-1}\}$ in Eq. (10) are the control points, i.e. points that only approximate the shape of the curve. The picked $\{L_j\}$ entities are points interpolating the curve, i.e. points that belong exactly to the curve. In order to build an exact representation of the curve, the control points set has to be computed from the interpolating points set. This evaluation can be performed solving a system of 3·*m* equations in 3·*m* unknowns (points $\{\mathrm{P}_i\}$ coordinates) imposing the passing of the curve through the *m* interpolating points $\{L_j\}$:

$$\left\{L_j\right\}=\sum_{i=0}^{m-1} b_i\left(u_j\right)\left\{\mathrm{P}_i\right\} \quad j=0..(m-1) \tag{20}$$

The values of the parameters u_j can be freely chosen. In order to built a smooth curve, a uniform distribution is suggested.

Figure 8 shows an example of geometry acquisition of a fragment. The user plays an important role in the activity because he chooses the location of interpolating points $\left\{L_j\right\}$ and their sequence. His action can be supported by the augmented reality system which superimposes graphical information to the scene in real time while they are sketched. Each acquired frame, the representation of the spline can be update and points and curves can be properly rendered.

Let consider a small fragment. First of all, in the acquisition of its shape is important to reconstruct the profile of its boundaries. Then, a series of curves can be sketched on the shell. If the surface presents some stripes or other peculiarities due to manufacturing, it is important to follow these geometrical features during the acquisition. In other cases, it cannot be important the acquisition of the entire surface of the object or of its boundaries, but only the sketching of some important feature (holes, profiles, etc.).

Each sketched curve can be used to built a mathematical spline representation. By this way, the augmented reality system guides the user during the whole acquisition operation. Thanks to the prospective collimation, if the user moves in the scene, the picked points and the corresponding curves are always rendered in the right position and collimated to the real objects.

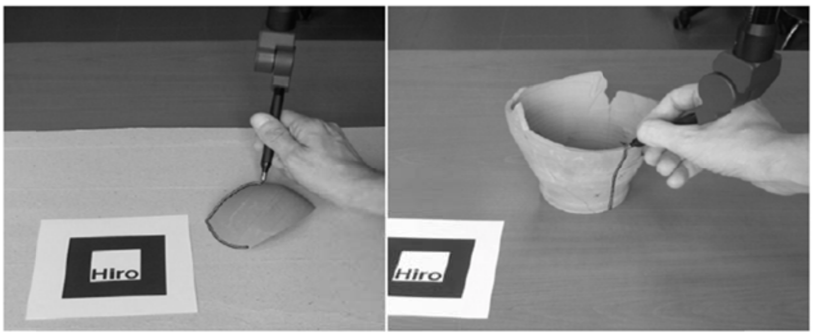

Figure 8. Interactive curve sketching in augmented reality on archaeological objects: an acquisition of edges on a small fragment (on the left) and of a profile on a portion of a vase (on the right).

After the acquisition and reconstruction of a set of curves on the interesting object, one of more surface patches can be generated. Two methods can be used. The first one involves the sketching of all the boundary curves of the object. If the real geometry is quite complicated or presents local features to be preserved [38], other internal curves can be sketched. Starting from this collection of curves, a control points net can be generated by interpolation among each curve control points [39] and a mathematical representation of a surface can be built as described in the previous section.

In Figure 9, an example of this strategy is depicted. In this case, the user has sketched four boundary curves and three internal curves. Starting from these choices, a surface patch is built.

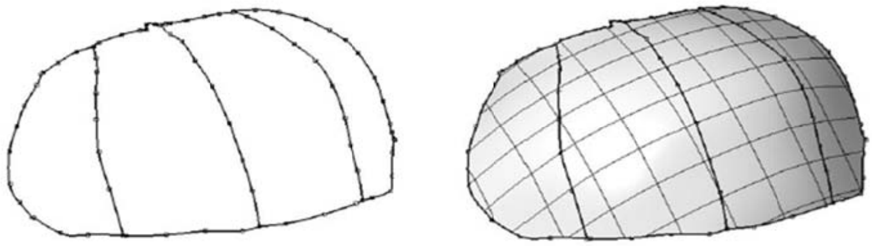

Figure 9. Building a surface patch starting from a collection of curves.

The surface can be also built following a second method. In this case the user has to sketch a series of profiles almost parallel. The final shape will be obtained as a loft between the profiles respecting the picking order. This second method is useful for large rectangular objects in which one dimension is greater than the others.

Figure 10 shows an example of a shard reconstructed using lofting technique.

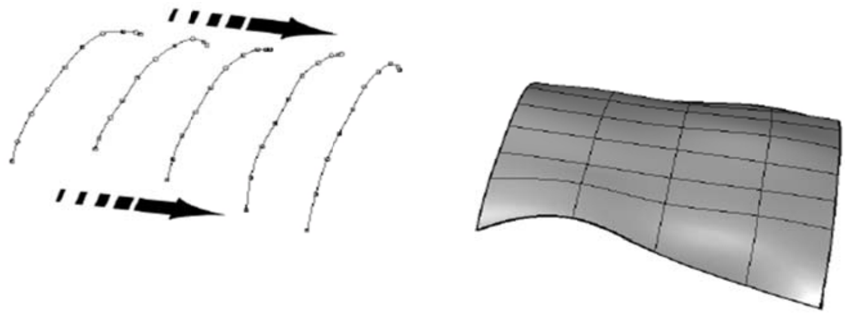

Figure 10. Building a surface loft starting from a series of profiles.

In Figure 11, the results of the mathematical reconstruction following the first strategy has been rendered in the augmented scene near the real fragment. It can be observed the very close similarity between the two shapes.

The similarity can be increased if the virtual object is colored with the same hue of the original shape. It is interesting to notice that, thanks to OpenGL capabilities, the texture of the real surface can be also optically acquired and rendered on the virtual replicas.

3.3. Geometrical Analysis of Fragments

The acquisition of curves and surfaces is important not only for a realistic virtual rendering of the shapes, but also for their interrogation [40], classification [41-42] and analysis [43-44]. The mathematical representation of geometrical entities is useful to apply the numerical algorithms typical of mathematics. Let us discuss some interesting cases.

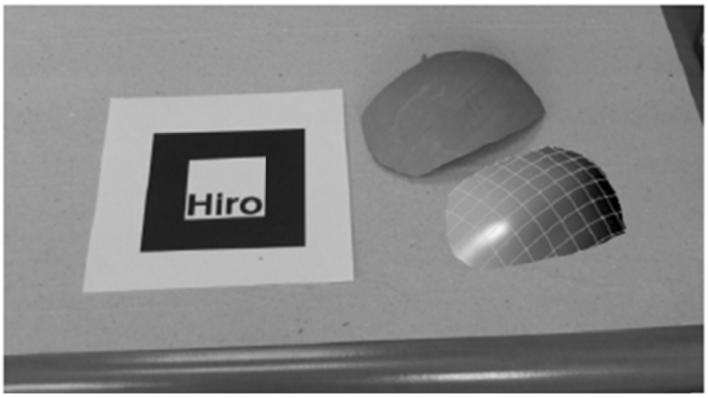

Figure 11. A virtual replica of a fragment placed near the real one in the augmented reality scene.

3.3.1. Study of Revolved Surfaces

Imagine that we want to investigate if a fragment belongs to a shapes that presents an axis of revolution. A typical example can be a portion of a vase or a cup. In this case, a manual estimation of this property is quite complex and it is more difficult if the fragment is very small. On the other side, in term of mathematical properties, this occurrence can be easily check. In general, a revolved surface has the Gaussian curvature constant along with parallels. A variation of this parameter can be observed only along meridians.

The Gaussian curvature *K* of a surface is defined [36] as:

$$K = \kappa_{\min} \cdot \kappa_{\max} \tag{21}$$

where $\kappa_{\min}$ and $\kappa_{\max}$ are the principal curvatures (the highest and the lowest values of surface curvature).

Since the reconstructed surface is only an approximation of the physical one, the distribution of the Gaussian curvature has to be evaluated considering a tolerance, especially near the boundaries where local perturbations may occur. Practically, this means that if the Gaussian curvature plot presents a series of stripes almost parallel, the surface is likely a part of a revolved shape. Figure 12 shows and example of this kind of investigation where the curvature plots are rendered on the virtual shape in order to easy visualize the topological property of the fragment surface.

Once the fragment has been considered a part of a revolved surface [45], it is possible to compute the approximated axis of revolution $\{d\}$. The unknown axis can be expressed in the parametric form as:

$$\{d\} = \{O\} + u \cdot \{n_0\} \tag{22}$$

where $\{O\}$ is a point belonging to the axis and $\{n_0\}$ is the direction unit vector.

Since in a revolved surface all the normal vectors pass through the axis of revolution, the unknown parameters $\{O\}$ and $\{n_0\}$ can be computed minimizing the following expression:

$$F = \sum_i \left| \frac{(P_i - O) \cdot (n_i - n_0)}{\|(n_i - n_0)\|} \right|^2 \tag{23}$$

where $\{n_0\}$ are the normal unit vectors computed for a collection of *i* sampling points P_i belonging to the surface.

The Eq. (23) expresses the residual of all the distances between all the normal vectors and the candidate axis of revolution. For this reason, Eq. (23) can be used for an alternative numerical method for understanding if the fragment is a part of a revolved surface. The surface can be considered of revolution only if the residual is below a specified tolerance.

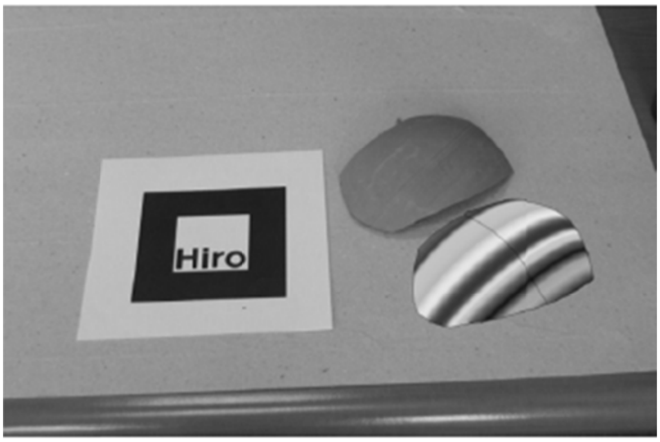

Figure 12. An example of curvature contours superimposed to the virtual replica of the fragment. From the interpretation of curvature plot it is possible to understand if the fragment is a part of a revolved surface.

3.3.2. Matching of Profiles

In many practical cases, it can be useful to perform a reconstruction of an entire shape starting from broken fragments. This activity can be performed using the mathematical representation of the shape in order to allow the use of numerical algorithms and reduce the risk of the manipulation of the delicate and precious parts. Moreover, if performed manually, this task is very time-consuming and requires a lot of patience for puzzling all the shapes.

In practical terms, two profiles match if they can be closely connected reproducing a continuous shape. Mathematically, this condition is fulfilled if it is possible to find a relative position between the two parts in which the distance between the two profiles is within a specified tolerance along the entire length.

Scientific literature presents several methods to check a possible matching between two profiles, based on deterministic, stochastic and heuristic methods. The check of compatibility between profiles is an important issue in many different research field as computer vision, geometric design and pattern recognition.

For the implementation in the augmented reality environment, we have to chose a method which is able to achieve results in real time and suitable for the introduced mathematical representation. In 1995 Lewis [46] proposed a method based on the use of cross correlation that has revealed to be fast and accurate. In 2005 the method has been enhanced by Cui et al. [47]. Following this approach, the matching between two curves can be checked computing the cross correlation between their geometrical invariants, i.e. topological properties that are not affected by geometrical transformation as rotation and translation. One of the most important geometrical invariant of a curve is the curvature [36]. The spline representation allows the robust computation of this parameter and the use of 3rd degree blending functions ensures an adequate curvature continuity.

Given two curves *a(u)* and *b(t)* the first step is to re-parameterize them considering the arc length *s*:

$$\begin{aligned} a(u) &\rightarrow a(s) \qquad s = \int_0^s \left\| a'(u) \right\| du \\ b(t) &\rightarrow b(s) \qquad s = \int_0^s \left\| b'(t) \right\| dt \end{aligned} \tag{24}$$

The spatial curvature $\kappa(s)$ for the two curves can be computed as:

$$\begin{aligned} a(s) &\rightarrow \kappa_a(s) = \frac{\partial^2 a(s)}{\partial s^2} \\ b(s) &\rightarrow \kappa_b(s) = \frac{\partial^2 b(s)}{\partial s^2} \end{aligned} \tag{25}$$

It is interesting to notice that Eq. (25) gives the same result of Eq. (14), but the relationship is deduced in term of arc-length.

The normalized cross correlation *CC* between the two curvature expressions along their entire length can be computed as:

$$CC(\kappa_a, \kappa_b) = \frac{\int (\kappa_a(s) \cdot \kappa_b(s)) ds}{\sqrt{\int \kappa_a(s) ds} \cdot \sqrt{\int \kappa_a(s) ds}} \tag{26}$$

The CC is a function in the range [-1..+1]. The more the curve are similar, the more the *CC* is near to 1.

In many cases involving fragments, the matching between two curves has to be checked only for a limited physical portion. It means that a curve *b(s)* has to be compatible to a part of the other curve *a(s)* only. In this case the correlation has to be computed with the corrected formula:

$$CC_{whole-to-part}(\kappa_a, \kappa_b) = \frac{\int \left(\kappa_a(s) \cdot \kappa_b(s - s^*)\right) ds}{\sqrt{\int \kappa_a(s) ds} \cdot \sqrt{\int \kappa_a(s - s^*) ds}} \tag{27}$$

in which the parameter *s** represents the offset of one curve with respect to the other one.

In this more frequent occurrence, we have to deal with different cross correlation values, in which the curve *a* can be considered as a template window sliding along the second curve *b*. In this case the best correlation is given for a specific value of the offset parameter *s**.

Recent contributions have introduced other methods for checking the congruency of profile based on stochastic, heuristic and Bayesian methods. A complete overview of these methodologies goes beyond the scope of this chapter and the interested reader can find further details in [48-51].

3.3.3. Profile Recognition and Database Comparison

The normalized cross correlation computed considering geometrical invariants can be used also for the comparison between an acquired profile and a database of reference shapes. In this case the problem is that the database shape are collected using reference dimensions that are usually scaled with respect to the real one. The curvature is not an invariant under the scaling operation, but it is affected by the same scale factor [47]. It means that a basic curve with a curvature κ when it is subjected to a scaling operation using an uniform scale factor *sf*, changes its curvature that becomes $\frac{\kappa}{sf}$.

In this case, the Eqs. (26) and (27) can be used for the comparison between two curves *a* and *b* after a normalization according to the scale factor. This normalization can be performed finding the highest value of both curvatures $\kappa_{a,\max}$ (maximum curvature value of profile *a*) and $\kappa_{b,\max}$ (maximum curvature value of profile *b*) and their ratio:

$$sf = \frac{\kappa_{a,\max}}{\kappa_{b,\max}} \tag{28}$$

as an esteem of the scale factor. Then, the comparison can be made computing the cross correlation between the corrected curvature values $\kappa_{a,\max}$ and $sf \cdot \kappa_{b,\max}$.

Figure 13 shows an example of profile analysis and database comparison.

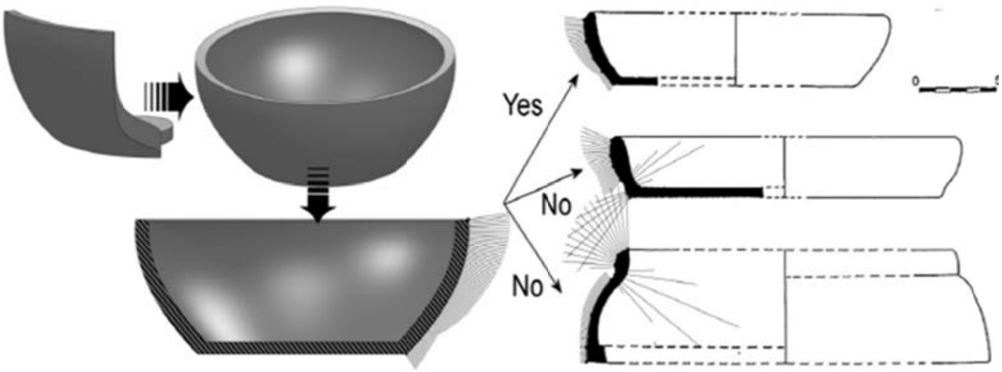

Figure 13. Comparison between reconstructed profile and database based on curvature correlation.

4. Interactive Manipulation of Virtual Objects

The geometrical representation of the acquired shapes can be also useful in order to have a virtual replica of the objects under investigation. The manipulation of virtual components it important for avoiding the risk of damage of the real ones and to perform some kind of analysis that are not possible on the real ones. Moreover, in many cases, the operations that can be performed with the virtual replicas cannot be executed on the real one at all. For example, a section of the geometry in order to analyze what is behind or inside an object it is not possible on the real object without breaking it. On the contrary, it is possible by using the mathematical representation and applying the proper transformations.

4.1. Adding Virtual Entities

The visualization during the manipulation of the reproduced shapes can be enhanced adding useful virtual entities to the scene. Symmetry axes, points, tripods, planes and curves are some example of these additional contents. They are useful for a spatial visualization of entities that do not exist in the real environment (and cannot be viewed in a real context) but are very important for the study of the geometrical properties of the objects under investigation. The rendering of overlay text can be also useful for including textual information in the scene, producing notes or interactive explanations.

4.2. Scaling and Magnifying Virtual Objects

One of the basic operation that can be performed on the virtual replicas of the real objects is the geometrical scaling. This action is useful to observe the shapes as under a magnifying lens. Since we have the mathematical representation of the surfaces, the scaling procedure is quite simple and can be performed by applying a transformation matrix to the equation of the surface:

$$s_{scaled}\left(u,v\right)=\left[T\right]_{scaling}\,s_{scaled}\left(u,v\right) \tag{29}$$

where:

$s\ \left(u,v\right)$ is the parametric representation of the surface to be scaled;

$s_{scaled}\left(u,v\right)$ is the parametric representation of the scaled surface;

$\left[T\right]_{scaling}$ is the homogeneous transformation matrix of the scaling operation that in case of uniform scaling with respect to the origin of the global reference frame can be set as:

$$\left[T\right]=\begin{bmatrix} sf & 0 & 0 & 0 \\ 0 & sf & 0 & 0 \\ 0 & 0 & sf & 0 \\ 0 & 0 & 0 & 1 \end{bmatrix} \tag{30}$$

in which the parameter sf is the scale factor.

4.3. Interactive Live Sectioning of Virtual Objects

Another interesting operation that can be performed on the virtual replicas of the real objects is the interactive sectioning of the geometry. With this action, the user can perform a geometrical cut of the acquired geometry using a virtual plane that can be moved by the user in real time. The operation can be implemented by limiting the rendering of the surface only to the portion that lay on one side of the cutting plane $cp\left(r,t\right)$. Mathematically this condition can be expressed by the following relationships:

$$\begin{aligned} &\text{distance}\left\{s\left(u_p,v_p\right),cp\left(r,t\right)\right\}\geq 0\rightarrow \textit{render}\ \text{point}\ s\left(u_p,v_p\right) \\ &\text{distance}\left\{s\left(u_p,v_p\right),cp\left(r,t\right)\right\}< 0\rightarrow \textit{skip}\ \text{point}\ s\left(u_p,v_p\right) \end{aligned} \tag{31}$$

The position and attitude of the cutting plane in the scene can be set and modified by the user interactively. This operation can be performed using the mechanical tracker. In this case the tip of the tracker can define the location in space of a point on the plane and its attitude the direction of its normal vector. By this way, if the user moves the tracker, the position and attitude of the cutting plane change accordingly.

Figure 14 shows an example of an interactive section of a virtual replica of a vase. The position and the attitude of the cutting plane are defined by the user using the tracker.

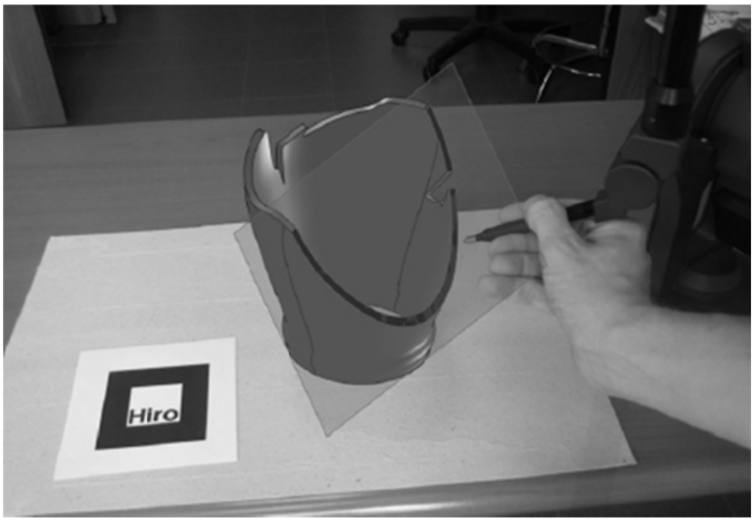

Figure 14. An example of interactive sectioning: the user moves the tracker and the cutting plane changes position and orientation and the geometry of the virtual component is sectioned accordingly (occlusions between cutting plane and real objects aren't take into account).

4.4. Free Moving and Rotating of Virtual Objects

In many cases it can be useful to manipulate the objects for observing from different points of view, comparing shapes and discovering details. The manipulation of virtual replicas can be safer than that on the real objects and the operation can be also combined with scaling or sectioning in order for improving the effectiveness.

The manipulation of the virtual objects can be assisted by the digitizer that allows a real time interaction. By this way, the digitizer can be used as an handle in order to grab, move and rotate the virtual objects. In order to deduce the algorithm for moving virtual components we can adapt the idea for mechanical assembling implemented and discussed in [19] as:

- The user can freely move the digitizer in the space. When it is close to a virtual object, he can pick the object. This occurrence can be checked computing the distance between the tip of the digitizer and the virtual surfaces in the scene. If the evaluated distance is smaller than a chosen tolerance, the digitizer can be considered in contact with the object.
- If the user confirms the picking, the virtual object becomes fixed to the digitizer. It means that its position and attitude depend on those of the digitizer.
- By moving the digitizer, the user moves the virtual object changing both position and attitude in space.
- The manipulation ends when the user decides to release the object which remains still till the next manipulation procedure begins.

Figure 15 shows an example of the manipulation of a virtual fragment attached to the digitizer tip in a scene with a real vase in order to optically check the congruency between the geometries.

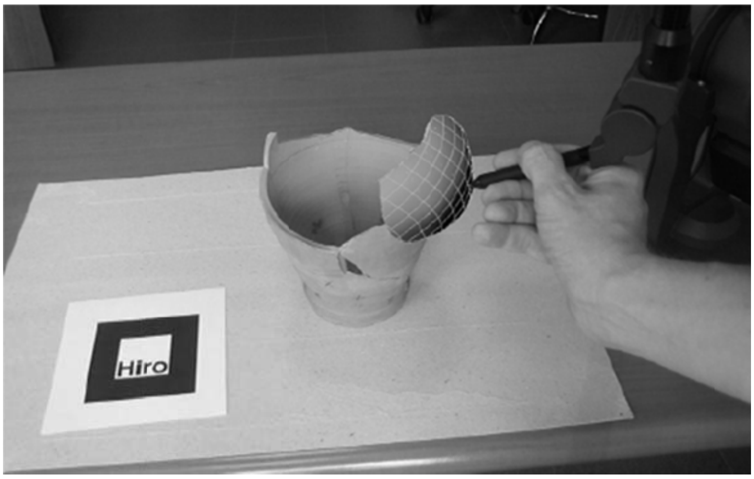

Figure 15. An example of the interactive manipulation of a virtual fragment in an augmented scene with a real vase.

4.5. Functional Constraints and Moving Partially Constrained Objects

The free moving of a virtual replica in the augmented scene can be helpful for many purposes. On the other hand, there are some cases in which it can be useful that the virtual object has some constrains in the scene and its motion is somehow limited. Consider, as an example, a fragment of a revolved surface (as those described in the previous section) that is going to be tested on a bigger part in order to understand if a reconstruction is possible. In this case the basic condition for a positive matching is that the revolving axis of both parts has to be the same. For this reason, in order to find the correct location, the relative position between the two parts has to be constrained with a functional relationship. For the specific case, it means that the fragment can be only rotated about the revolving axis and/or translated along it (and eventually flipped) [52].

The presence of the functional constraints has several implications for the augmented reality implementation. First of all, the functional entities (such as the revolving axes) have to be rendered in the scene in order to make them evident. Secondly, it has to be possible to snap those entities using proximity functions. Thirdly, a procedure for dealing with the interactive placement of partially constrained object has to be implemented.

A possible solution to this last problem can be derived from that used for managing assembling procedure in augmented reality and discussed by Valentini in [19]. A generic constraint imposed on a virtual object can be represented by one of more equations as:

$$\left\{\Psi_{\text{constraint}}\right\} = \left\{0\right\} \tag{32}$$

In the same way, the condition that the virtual object has to move fixed to the digitizer tip position and attitude can be imposed with 6 scalar equations:

$$\left\{\Psi_{\text{digitizer}}\right\} = \left\{0\right\} \tag{33}$$

Considering that the constraint equations in (32) are mandatory and those in (33) are used only for the achieving a good level of interaction, the motion of a partially constrained virtual part subjected to the user's grabbing can be computed solving the relationship:

$$\begin{cases} \left\{\Psi_{\text{constraint}}\right\} = \left\{0\right\} \\ \min\limits_{\text{position and attitude}} \left\| \left\{\Psi_{\text{digitizer}}\right\} \right\| \end{cases} \tag{34}$$

Figure 16 shows a possible sequence for the implementation of the functional constraint manipulation algorithm. At the beginning of the manipulation, the shards is free to be moved in the space and its position and attitude are constrained by the digitizer. When the axis of the fragment is near (within a tolerance) to that of the vase a functional constraint can be enforced (the two axes have to be coincident). From this moment, the shard can be moved respecting Eqs. (34) around the common axis and/or along it. During the manipulation, if two parts came in contact (the distance between two boundary curves is lower than a specific tolerance), the compatibility between the two boundary profiles can be real time evaluated using Eq. (27) and a graphical results can be rendered in the scene in order to underline a possible positive matching.

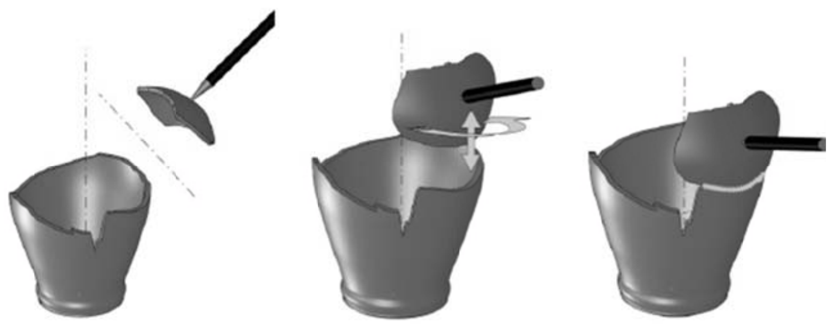

Figure 16. Moving and positioning virtual shard using functional constraints.

5. CONCLUSION

The use of augmented reality in combination with modeling and reverse engineering methodologies has revealed to be very useful for supporting the user in many phases of the study of cultural and archaeological artifacts.

The integration of the reverse engineering tools into an augmented reality environment has been achieved using a digitizer arm which has been synchronized and collimated to the projection of the virtual scene. This embodiment allows the implementation of interactive procedures in which the user can operate in real time, producing 3D sketches, measuring geometries, manipulating objects, matching shapes, etc. By this way all the reverse engineering activities from the acquisition of the shapes to their interrogation and reconstruction can be performed with the help of realistic computer graphic contents directly superimposed to the real scene in a mixed real-virtual environment. The use of the digitizer can be assimilated to the use of a special pen whose tip position can be tracked and recorded is a three dimensional space.

The entire implementation has been programmed using open source libraries and this feature allows simpler development for further investigations.

REFERENCES

[1] Forte M., Siliotti A., Renfrew C. (eds.) (1997) *Virtual Archaeology: Re-Creating Ancient Worlds*. New York: Harry N. Abrams.

[2] Su C.J., Yen, Benjamin P.C., Zhang, X. (1998) An internet based virtual exhibition system: Conceptual design and infrastructure, *Computers and Industrial Engineering*, 35:3-4, pp. 615-618.

[3] Winterbottom, S.J.; Long, D., (2006) From abstract digital models to rich virtual environments: landscape contexts in Kilmartin Glen, Scotland, *Journal of Archaeological Science* Volume: 33: 10, pp. 1356-1367.

[4] Lutz W., (1999) Cultural Heritage: Virtual Dunhuang Art Cave: A Cave within a CAVE, *Computer Graphics Forum* Volume: 18:3, pp. 257-264.

[5] Price A., (2003) Interactive Virtual Reconstructions: Visualization and User Interface Design for Installations in Public Venues. *Proc. of the Seventh International Conference on Information Visualization* (IV'03) 1093 9547/03.

[6] Ioannides, M., Wehr, A. (2002) 3D-Reconstruction & Re-Production in Archaeology. *Proc. of International Workshop on Scanning for Cultural Heritage Recording*, Sept. 1-2, Corfu, Greece.

[7] Cosmas J., Itagaki T., Green D., Grabczewski E., Waelkens M., Degeest R., et al. (2001). 3D MURALE: A Multimedia System for Archaeology. *Proc. ACM Virtual Reality, Archaeology and Cultural Heritage* .

[8] Kirchner S., Jablonka P., (2001) Virtual Archaeology - VR based knowledge management and marketing in archaeology first results - nexts steps, *Proc. of the 2001 Conference on Virtual reality, archeology, and cultural heritage* Glyfada, Greece.

[9] Pennestrì E., Pezzuti E., Valentini P.P., Vita L., (2006) Computer Aided Reconstruction of Italian Ancient Clocks, *Computer Animation and Virtual World*, vol. 17, pp.565-572.

[10] Azuma R.T. (1997). A survey of augmented reality. *Teleoperators and Virtual Environments*, 6(4), pp. 355-385.

[11] Bimber O., Raskar R. (2005). *Spatial Augmented Reality: Merging Real and Virtual Worlds*, A K Peters, Ltd.

[12] Azuma R., Baillot Y. et al. (2001). Recent advances in augmented reality. *IEEE Computer Graphics* 21(6), pp. 34-47.

[13] Liarokapis F. (2007). An augmented reality interface for visualizing and interacting with virtual content, *Virtual Reality* 11, pp. 23-43.

[14] Samset E., Talsma A., Elle O., Aurdal L., Hirschberg H., Fosse E. (2002). A virtual environment for surgical image guidance in intraoperative MRI, *Computer Aided Surgery* 7(4), pp.187– 196.

[15] Stilman M., Michel P., Chestnutt J., Nishiwaki K., Kagami S., Kuffner J.J. (2005). *Augmented Reality for Robot Development and Experimentation*. Tech. Report CMU-RI-TR-05-55, Robotics Institute, Carnegie Mellon University.

[16] Ong S.K., Pang Y., Nee, A.Y.C. (2007). Augmented Reality Aided Assembly Design and Planning. *Annals of the CIRP* Vol. 56/1 pp.49-52.

[17] Pang Y., Nee A.Y.C., Ong S.K., Yuan M.L. Youcef-Toumi K. (2006). Assembly Feature Design in an Augmented Reality Environment, *Assembly Automation*, 26/1, pp. 34-43.

[18] Sharma R. and Molineros J. (1995). Computer vision-based augmented reality for guiding manual assembly. *PRESENCE: Teleoperators and Virtual Environments*, n. 3, pp. 292-317.

[19] Valentini P.P. (2009), Interactive virtual assembling in augmented reality, *International Journal on Interactive Design and Manufacturing* vol. 3, 2009, pp. 109-119.

[20] Webster A., Feiner S., MacIntyre B., Massie W., Krueger T. (1996). *Augmented reality in architectural construction, inspection, and renovation*. Int. Proc. Of Third Congress on Computing in Civil Engineering ASCE 3, Anaheim, CA, pp. 913-919.

[21] Liarokapis, Petridis P., Lister P.F., White M. (2002). Multimedia augmented reality interface for E-learning (MARIE*). World TransEng Technol Educ* 1(2), pp.173–176.

[22] Pan Z., Cheok A.D., Yang H., Zhu J.,_, Shi J. (2006). Virtual reality and mixed reality for virtual learning environments. *Computers & Graphics* 30, pp. 20–28.

[23] Dangelmaier W., Fischer M., Gausemeier J., Grafe M., Matysczok C., Mueck B. (2005). Virtual and augmented reality support for discrete manufacturing system simulation. *Computers in Industry* 56, pp. 371–383.

[24] Ong S.K., Nee A.Y.C. (2004). *Virtual and Augmented Reality Applications in Manufacturing*. Springer, London, UK.

[25] Reif R., Walch D. (2008). Augmented & Virtual Reality applications in the field of logistics. *Visual Computing* 24, pp. 987–994.

[26] Friedrich W. (2004). *ARVIKA—Augmented Reality for Development, Production and Service*. Publicis Corporate Publishing, Erlangen.

[27] Narzt W., Pomberger G., Ferscha A., Kolb D., Muller R, Wieghardt J., Hortner H., Lindinger C. (2006). Augmented reality navigation systems. *Univ Access Inf Soc* 4, pp. 177–187.

[28] Valentini P.P., Pezzuti E., Gattamelata D. (2010), Virtual engineering in augmented reality, chapter in Computer Animation, series “Computer Science, Technology and Applications”, Nova Science Publisher Inc. , New York, pp. 57-83.

[29] Valentini P.P., Pezzuti E., (2010) Interactive Multibody Simulation in Augmented Reality, *Journal of Theoretical and Applied Mechanics*, vol 48, n.3, pp. 733-750.

[30] Liarokapis F., Sylaiou S., et al. (2004). An interactive visualization interface for virtual museum. *Proc. of the 5th international symposium on Virtual Reality, Archaeology-Cultural Heritage*, Brussels and Oudenaarde, pp 47-56.

[31] Wojciechowski R., Walczak K., White M., Cellary W., (2004) Building Virtual and Augmented Reality museum exhibitions, *Proc. of the 9th international conference on 3D Web technology*, Monterey, California.

[32] Kathryn A. I., (1994). *Reverse Engineering*, McGraw-Hill Inc.

[33] Morel J.P. (1981). *Céramique campanienne: les formes*, Rome (in French).

[34] Shepard A. (1965). *Ceramics for the Archaeologist*, Washington.

[35] Whittaker J.C. et. al. (1998). Evaluating consistency in typology and classification, *J. of Archaeological Method and Theory*, 5, 2: pp. 129-164.

[36] Farin G. (2002). *Curves and Surfaces for CAGD, a practical guide*. Morgan-Kaufmann, 5th edition.

[37] Paoluzzi A. (2003) *Geometric Programming for Computer-Aided Design*, Wiley.

[38] Kammerer P., Mara H., Kratzmüller B., Zolda E. (2005). Detection and analysis of lines on the surface of archaeological pottery, in V. Cappelini & J. Hemsley (eds.), *Electronic Imaging and the Visual Arts*, Florence/Bologna, Pitagora ed. pp. 154-159.

[39] Levin A., (1999) Interpolating nets of curves by smooth subdivision surfaces in *Proc. of SIGGRAPH 1999*, pp. 57-64.

[40] Kampel M., Sablatnig R. (2006). 3D Data Retrieval of Archaeological Pottery, *Interactive Technologies and Sociotechnical Systems* - Springer, Berlin.

[41] Gilboa A., Karasik A., Sharon I., Smilansky U. (2004). Towards computerized typology and classification of ceramics, *Journal of Archaeological Science* 31, pp. 681-694.

[42] Maiza C., Gaildrat V., (2005). Automatic classification of archaeological potsherds, Proc. of. the Eight Intern. Conf. on Computer Graphics and Artificial Intelligence, Limoges, France, May 11-12.

[43] Kampel M., Sablatnig R. (2002). Automated Segmentation of Archaeological Profiles or Classification, Proc. of the 16th Intl. Conf. on Pattern Recognition, Technische Univ. Wien, Vienna, Austria.

[44] Saragusti I., Karasik A., Sharon I., Smilansky U. (2005). Quantitative analysis of shape attributes based on contours and section profiles in archaeological research, *Journal of Archaeological Science* 32/6: pp. 841-853.

[45] Hörr C., Brunner D., Brunnett G. (2007). Feature Extraction on Axially Symmetric Pottery for Hierarchical Classification, *Computer-Aided Design & Applications*, 4:1-4 pp. 375-384.

[46] Lewis J.P. (1995). Fast normalized cross-correlation. In: *Vision Interface*. Canadian Image Processing and Pattern Recognition Society, pp. 120–123.

[47] Cui M., Femiani J., Hu J., Wonka P., Razdan A. (2009). Curve matching for open 2D curves. *Pattern Recognition Letters*, 30, pp. 1–10.

[48] Willis A., Cooper D.B. (2004). Bayesian assembly of 3D axially symmetric shapes from fragments, Proc. of the 2004 IEEE Computer Society Conference on Computer Vision and Pattern Recognition/CVPR 2004 (27 June-2 July), vol. 1, Washington: Institute of Electrical and Electronic Engineers: pp. 82-89.

[49] Ucoluk G., Toroslu I. (1999). Automatic reconstruction of broken 3-D surface objects. *Computers and Graphics*, 23(4) pp. 573-582.

[50] Gruen A., Akca D. (2001) Least squares 3D surface and curve matching, *ISPRS Journal of Photogrammetry & Remote Sensing*, 59, pp. 151– 174.

[51] Willis A.R. (2004). *Stochastic 3D Geometric Models for Classification, Deformation, and Estimation*, Doctoral dissertation, Division of Engineering at Brown University, Providence, Rhode Island, U.S.A.

[52] Kampel M., Sablatnig R. (2004). On 3D mosaicing of rotationally symmetric ceramic fragments, Proc. of the 17*th* International Conference on Pattern Recognition,

Cambridge, U.K., vol. 2, Cambridge: Institute of Electrical and Electronics Engineers Computer Society: pp. 265-268.